AFRL-RB-WP-TP-2011-3104

ALTITUDE CONTROL OF A SINGLE DEGREE OF FREEDOM FLAPPING WING MICRO AIR VEHICLE (POSTPRINT)

David B. Doman, Michael W. Oppenheimer, Michael A. Bolender, and David O. Sigthorsson

Control Design and Analysis Branch
Control Sciences Division

AUGUST 2009

AIR FORCE RESEARCH LABORATORY
AIR VEHICLES DIRECTORATE
WRIGHT-PATTERSON AIR FORCE BASE, OH 45433-7542
AIR FORCE MATERIEL COMMAND
UNITED STATES AIR FORCE

REPORT DOCUMENTATION PAGE

Form Approved
OMB No. 0704-0188

1. REPORT DATE *(DD-MM-YY)*	2. REPORT TYPE	3. DATES COVERED *(From - To)*
August 2009	Conference Paper Postprint	05 November 2008 – 13 August 2009

4. TITLE AND SUBTITLE
ALTITUDE CONTROL OF A SINGLE DEGREE OF FREEDOM FLAPPING WING MICRO AIR VEHICLE (POSTPRINT)

5a. CONTRACT NUMBER
In-house

5b. GRANT NUMBER

5c. PROGRAM ELEMENT NUMBER
62201F

6. AUTHOR(S)
David B. Doman, Michael W. Oppenheimer, Michael A. Bolender,
and David O. Sigthorsson (AFRL/RBCA)

5d. PROJECT NUMBER
2401

5e. TASK NUMBER
N/A

5f. WORK UNIT NUMBER
Q12K

7. PERFORMING ORGANIZATION NAME(S) AND ADDRESS(ES)
Control Design and Analysis Branch (AFRL/RBCA)
Control Sciences Division
Air Force Research Laboratory, Air Vehicles Directorate
Wright-Patterson Air Force Base, OH 45433-7542
Air Force Materiel Command, United States Air Force

8. PERFORMING ORGANIZATION REPORT NUMBER
AFRL-RB-WP-TP-2011-3104

9. SPONSORING/MONITORING AGENCY NAME(S) AND ADDRESS(ES)
Air Force Research Laboratory
Air Vehicles Directorate
Wright-Patterson Air Force Base, OH 45433-7742
Air Force Materiel Command
United States Air Force

10. SPONSORING/MONITORING AGENCY ACRONYM(S)
AFRL/RBSD

11. SPONSORING/MONITORING AGENCY REPORT NUMBER(S)
AFRL-RB-WP-TP-2011-3104

12. DISTRIBUTION/AVAILABILITY STATEMENT
Approved for public release; distribution unlimited.

13. SUPPLEMENTARY NOTES
PAO Case Number: 88ABW-2009-3332; Clearance Date: 21 Jul 2009. Document contains color.

Conference paper published in the proceedings of the AIAA Guidance, Navigation, and Control Conference held 10 - 13 August 2009 in Chicago, IL.

14. ABSTRACT
A control strategy is proposed for a minimally actuated flapping wing micro air vehicle. The Harvard RoboFly vehicle accomplished the first takeoff of an insect scale flapping wing aircraft. This flight demonstrated the capability of the aircraft to accelerate vertically while being constrained by guide-wires to avoid translation and rotation in the other five degrees of freedom. The present work proposes an altitude control scheme that would enable a similar vehicle under the same constraints to hover and track altitude commands. Using a blade element-based aerodynamic model and cycle averaging, it will be shown that altitude control of such an aircraft can be achieved. The RoboFly makes use of a single bimorph piezoelectric actuator that symmetrically varies the angular displacement of the left and right wings in the stroke plane. The wing angle-of-attack variation is passive and is a function of the instantaneous angular velocity of the wing in the stroke plane. The control law is designed to vary the frequency of the wing beat oscillations to control the longitudinal body-axis force which is used to achieve force equilibrium in hover and acceleration when tracking time-varying altitude commands.

15. SUBJECT TERMS
flapping wing micro air vehicles, MAV, minimal actuation, altitude control

16. SECURITY CLASSIFICATION OF:			17. LIMITATION OF ABSTRACT:	18. NUMBER OF PAGES	19a. NAME OF RESPONSIBLE PERSON (Monitor)
a. REPORT	b. ABSTRACT	c. THIS PAGE			1Lt Zachary H. Goff
Unclassified	Unclassified	Unclassified	SAR	26	19b. TELEPHONE NUMBER *(Include Area Code)* N/A

AIAA Guidance, Navigation, and Control Conference
10 - 13 August 2009, Chicago, Illinois

AIAA 2009-6159

Altitude Control of a Single Degree of Freedom Flapping Wing Micro Air Vehicle

David B. Doman *, Michael W. Oppenheimer †, Michael A. Bolender ‡and David O. Sigthorsson §

A control strategy is proposed for a minimally actuated flapping wing micro air vehicle. The Harvard RoboFly vehicle accomplished the first takeoff of an insect scale flapping wing aircraft. This flight demonstrated the capability of the aircraft to accelerate vertically while being constrained by guide-wires to avoid translation and rotation in the other five degrees of freedom. The present work proposes an altitude control scheme that would enable a similar vehicle under the same constraints to hover and track altitude commands. Using a blade element-based aerodynamic model and cycle averaging, it will be shown that altitude control of such an aircraft can be achieved. The RoboFly makes use of a single bimorph piezoelectric actuator that symmetrically varies the angular displacement of the left and right wings in the stroke plane. The wing angle-of-attack variation is passive and is a function of the instantaneous angular velocity of the wing in the stroke plane. The control law is designed to vary the frequency of the wing beat oscillations to control the longitudinal body-axis force which is used to achieve force equilibrium in hover and acceleration when tracking time-varying altitude commands.

*Senior Aerospace Engineer, Control Design and Analysis Branch, 2210 Eighth Street, Ste. 21, Air Force Research Laboratory, WPAFB, OH 45433-7531 Email David.Doman@wpafb.af.mil, Ph. (937) 255-8451, Fax (937) 656-4000, Associate Fellow AIAA

†Senior Electronics Engineer, Control Design and Analysis Branch, 2210 Eighth Street, Ste 21, Air Force Research Laboratory, WPAFB, OH 45433-7531 Email Michael.Oppenheimer@wpafb.af.mil, Ph. (937) 255-8490, Fax (937) 656-4000, Senior Member AIAA

‡Aerospace Engineer, Control Design and Analysis Branch, 2210 Eighth Street, Ste 21, Air Force Research Laboratory, WPAFB, OH 45433-7531 Email michael.bolender@wpafb.af.mil, Ph. (937) 255-8492, Fax (937) 656-4000, Senior Member AIAA

§Electronics Engineer, Control Design and Analysis Branch, 2210 Eighth Street, Ste 21, Air Force Research Laboratory, WPAFB, OH 45433-7531 Email David.Sigthorsson@afmcx.net, Ph. (937) 255-9707, Fax (937) 656-4000. This research was performed while this author held a National Research Council Research Associateship Award at the Air Force Research Laboratory.

I. Introduction

The first takeoff of an insect scale biomimetic flapping wing micro air vehicle was achieved by an aircraft called RoboFly that was developed at Harvard University by Wood et.al.[1] A key feature that led to the successful first flight is that the vehicle is minimally actuated and makes use of passive wing rotation to mimic the wing beat patterns of a dipterian insect. As shown in Figure 1, RoboFly uses a single bimorph piezoelectric actuator to impart symmetric motion to two wings simultaneously. Tangential motion of the tip of the piezoelectric actuator is converted to rotational motion of the wings by way of a linkage. The linkage elements are designed to achieve impedance matching between the wing and actuator forces and to amplify the relatively small motion of the tip of the bimorph strip into large angular displacements of the wing in the stroke plane. A wing is connected to the movable wing root by a flexible hinge that provides for passive rotation of the wing. The hinge allows the wing to passively invert its orientation about the hinge joint as the wing reverses direction at the end of each stroke. This results in planform rotations that approximate the motion of dipterian insect wings. As the wing traverses through the stroke plane, dynamic pressure acting on the wing tends to cause it feather into the wind; however, as shown in Figure 2, the hinge joint is designed for interference between the planform and root to prevent the wing from over-rotating. Therefore, the wing holds a constant angle of attack relative to the stroke plane once a critical dynamic pressure is reached. The actuator and the carbon fiber substrate to which it is mounted are cantilevered to the fuselage and together with the wing form a spring-mass-damper system that has a known resonant frequency. In the Harvard experiment, this dynamic system was driven at resonance for maximum energy efficiency to achieve flight. The first flight resulted in unregulated flight up a wire that constrained the vehicle motion to vertical translation. In the first part of this paper, we investigate the suitability of wingbeat frequency modulation to allow tracking of a desired vertical position profile of the single degree of freedom (DOF) RoboFly experiment. In the companion pair of papers,[2,3] a vehicle concept and associated control strategies that will allow the vehicle to break free of the wire and allow controlled six degree of freedom flight of the fuselage is explored.

II. Single Degree of Freedom Dynamic Model of RoboFly

The first flight of the Harvard RoboFly was conducted by constraining the aircraft to vertical translation on a pair of wires. Here, the motion of the RoboFly fuselage acting under the influence of a time varying vertical aerodynamic force that is a function of the wingbeat motion is modeled. The wings represent about 1% of the total vehicle weight and

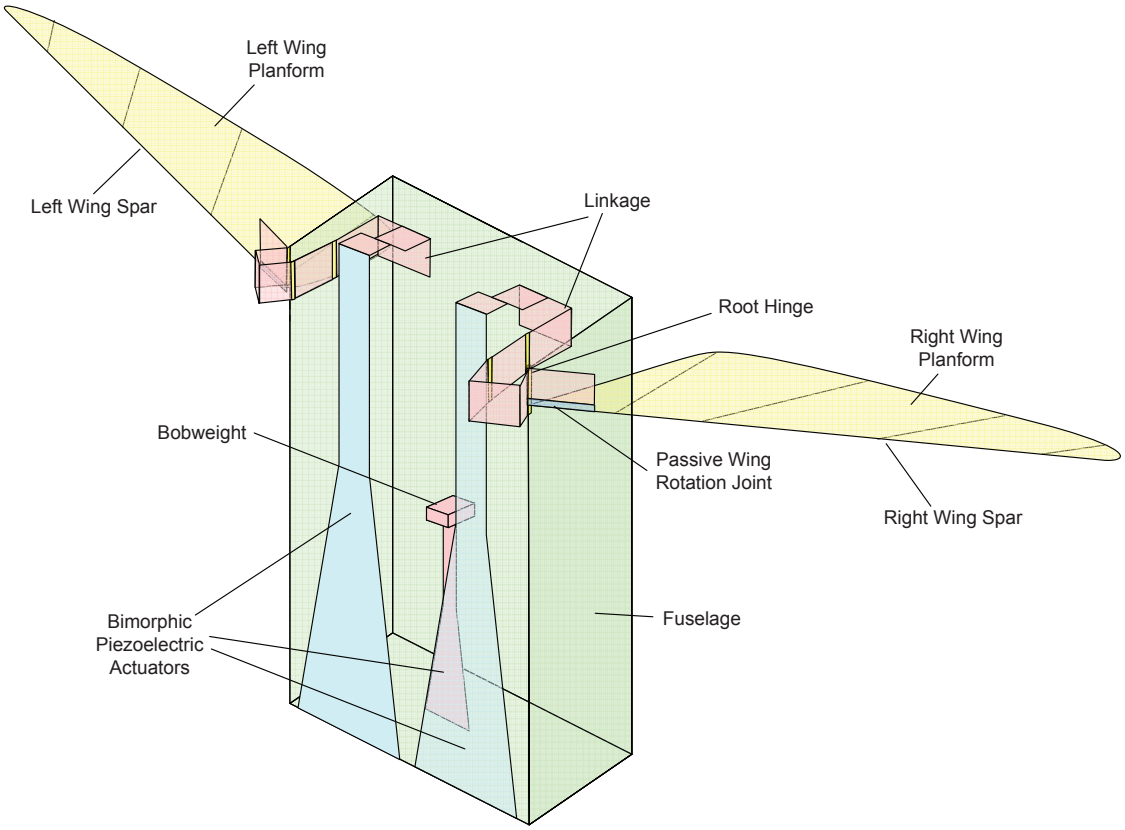

Figure 1. General assembly drawing of Harvard RoboFly.

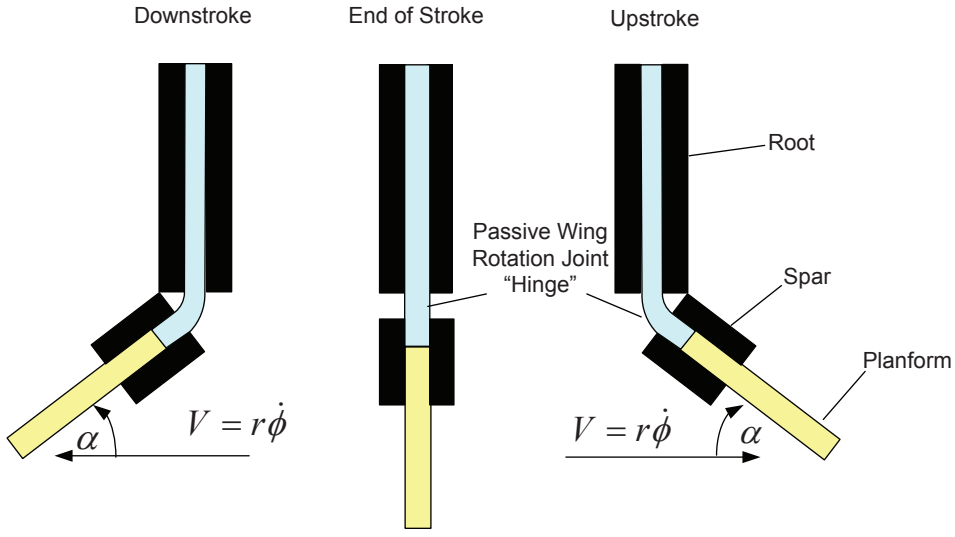

Figure 2. Detail of passive wing rotation joint.

are assumed to be massless for the purpose of this analysis. The equation of motion for the

1 DOF Robofly is simply

$$F_x(t) = m(\ddot{x} + g) \tag{1}$$

where x lies along a unit vector x_I in an inertial frame that is taken to be positive away from the center of the earth. The aerodynamic force in the x_I direction is derived using blade element theory for a triangular shaped wing that has two degrees of freedom, namely angular displacement, $\phi(t)$, about the wing root in the stroke plane, which is normal to the body x-axis x_B, and angular displacement about the passive rotation hinge joint, which is equivalent to wing angle-of-attack α in still air. The triangular planform wing shown in Figure 3 is taken to be a rigid flat plate whose elemental lift at a spanwise location in the local wing planform plane is given by

$$dL = \frac{\rho}{2} C_L(\alpha) \dot{\phi}^2 y_{WP}^2 c(y_{WP}) dy_{WP} \tag{2}$$

$$dD = \frac{\rho}{2} C_D(\alpha) \dot{\phi}^2 y_{WP}^2 c(y_{WP}) dy_{WP} \tag{3}$$

where $c(y_{WP})$ is the chord at the spanwise location y_{WP}, which is a location on the wing spar. The total lift and drag on the wing expressed in a wing planform fixed coordinate system, e.g., RWPU, RWPD, LWPU, and LWPD is now computed, where RWPD is the right wing planform coordinate system for the downstroke, RWPU is the right wing planform coordinate system for the upstroke, and similarly for the left wing. Such a coordinate frame has an origin at the wing root hinge point and its x-y plane is coincident with the wing planform. The lift

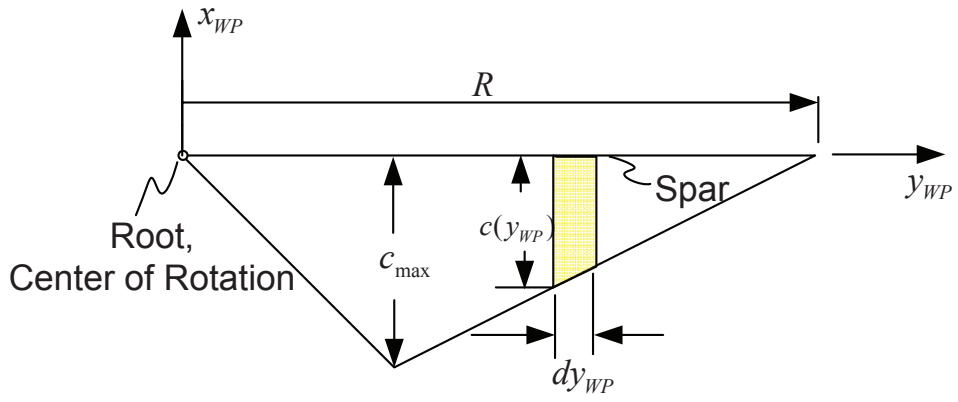

Figure 3. Blade element computation of aerodynamic forces, moments and centers of pressure.

is computed by integrating the elemental lift over the span according to

$$L = \int_0^R dL = \frac{\rho}{2} C_L(\alpha) \dot{\phi}(t)^2 I_A \tag{4}$$

Similarly, drag is computed according to

$$D = \int_0^R dD = \frac{\rho}{2} C_D(\alpha) \dot{\phi}(t)^2 I_A \tag{5}$$

where I_A is the area moment of inertia of the planform about the root and R is the length of the wing.

Experiments by Sane and Dickenson[4] for a dynamically scaled model of a flapping insect show that while quasi-steady estimates fail to capture the temporal variation in lift over a stroke cycle, it does capture the the cycle averaged lift with reasonable accuracy. Best fit estimates of quasi-steady lift and drag coefficients derived from measurements acquired from 180^o sweeps of wing motion as a function of angle of attack are given by

$$\begin{aligned} C_L &= 0.225 + 1.58 \sin(2.13\alpha - 7.2) \\ C_D &= 1.92 - 1.55 \cos(2.04\alpha - 9.82) \end{aligned} \tag{6}$$

where α in Equation 6 is in degrees. For convenience, all of the time invariant parameters are lumped together according to

$$\begin{aligned} k_L &\triangleq \frac{\rho}{2} C_L(\alpha) I_A \\ k_D &\triangleq \frac{\rho}{2} C_D(\alpha) I_A \end{aligned} \tag{7}$$

Thus, lift and drag can be expressed as the product of time invariant parameters and time varying functions

$$\begin{aligned} L &= k_L \dot{\phi}(t)^2 \\ D &= k_D \dot{\phi}(t)^2 \end{aligned} \tag{8}$$

Note that the only variable that can be actively manipulated to control the instantaneous aerodynamic forces is the angular velocity of the wing, $\dot{\phi}(t)$, and the forces are quadratic functions of this motion variable. Furthermore, because the vehicle is designed to mimic dipterian insect flight, $\dot{\phi}(t)$ must be a time varying function that is equal to zero at the extreme limits of wing position. It is assumed that one can directly control the wing position. This assumption approximates the physics of applying a voltage to an actuator that induces a strain in the carbon fiber substrate that pushes and pulls on rigid linkage elements that translate the tip motion of the bimorph strip into rotational motion of the wing root. The forcing function that drives the wing rotation is

$$\phi(t) = \cos \omega t \tag{9}$$

Assuming that the frequency of the oscillating wing is held constant over each wingbeat cycle, the angular velocity of the wing is given by

$$\dot{\phi}(t) = -\omega \sin \omega t \tag{10}$$

Note that the units of $\phi(t)$ are radians and that the amplitude of the wing rotation in the stroke plane is 1 rad. The frequency of the oscillator that drives the actuator is the control input variable. The proposed control strategy is based on the assumption that the gain crossover frequency of the fuselage controller is much less than the trim flapping frequency required for hover. If a non-oscillatory control force were available and altitude and altitude rate measurements were available for feedback, one could simply implement a linear feedback control law that produced the response of a damped harmonic oscillator. But since the system is constrained to use time varying high frequency oscillatory control inputs, the relationship between the time averaged vertical force and the control input is computed. Also note that wing angle of attack is a function of the wing rotation rate because of the passive wing rotation joint discussed earlier.

A. Expression of Aerodynamic Forces in Body Axis Coordinate System

Six axis systems are defined to aid in mapping the lift and drag forces acting in the plane of the wing into body axis coordinates. The coordinate systems are body, inertial, right wing planform, right wing spar, left wing planform, and left wing spar. As shown in Figure 4, a body fixed axis system. x_B, y_B, z_B, is defined whose origin is located at the center of gravity of the fuselage. The x body axis lies in the plane of symmetry of the fuselage and the y body axis points out the right hand side of the vehicle, while the z body axis points out the ventral side of the MAV. A right wing root fixed frame, $x_{RWR}, y_{RWR}, z_{RWR}$, is defined that is aligned with x_B, y_B, z_B but whose origin is located at the right wing root pivot point. A right wing spar fixed frame, $x_{RWS}, y_{RWS}, z_{RWS}$, is defined that rotates through an angle $\phi(t)$ about the root pivot point. Here, when $\phi(t) = 0$, $z_{RWS} = -x_{RWR}$, y_{RWS} is coincident with the wing spar, and z_{RWS} completes the right handed coordinate system. The transformation between the spar and root axis system is given by

$$\begin{bmatrix} x_{RWR} \\ y_{RWR} \\ z_{RWR} \end{bmatrix} = \begin{bmatrix} 0 & 0 & -1 \\ -\sin\phi(t) & \cos\phi(t) & 0 \\ \cos\phi(t) & \sin\phi(t) & 0 \end{bmatrix} \begin{bmatrix} x_{RWS} \\ y_{RWS} \\ z_{RWS} \end{bmatrix} \tag{11}$$

The right wing planform frame rotates about the leading edge spar by an angle α which corresponds to the wing angle of attack when the vehicle is at hover in a quiescent air mass.

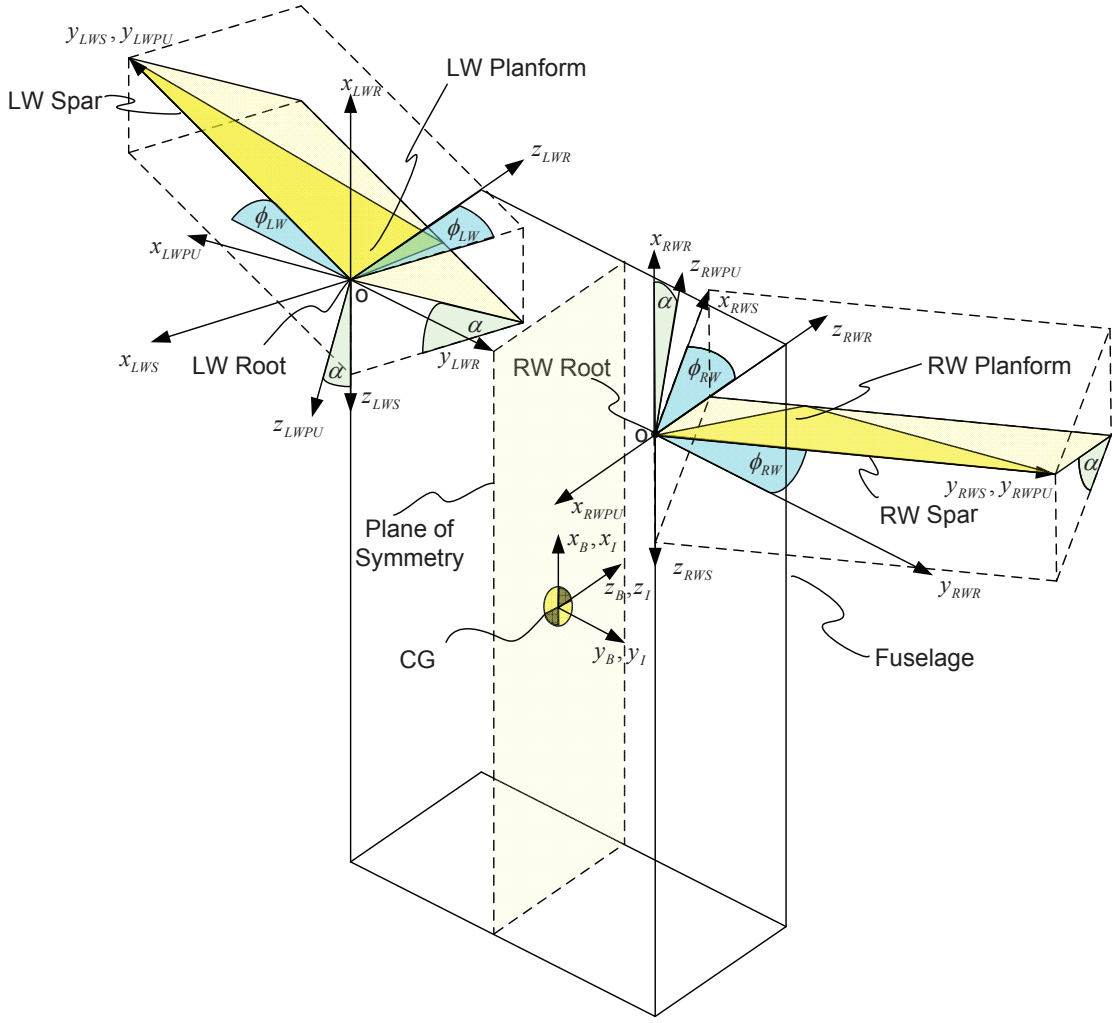

Figure 4. Relationship between, inertial, body, root, spar, and wing planform axis systems.

The wing plane rotates about an ideal hinge located at the spar-root hinge point. As the wing rotates about the root pivot point, dynamic pressure acting on the wing causes it to feather into a direction parallel to the stroke plane; however, the magnitude of the rotation is limited by the design of the joint as illustrated in Figure 2. When $\dot{\phi}(t) = 0$ the wing hangs vertically, i.e., $\alpha = 90^o$, under the influence of gravity alone. On the downstroke of the right-hand wing, $\dot{\phi}(t) > 0$ and when sufficient dynamic pressure is achieved to engage the hinge stop, $\alpha = \alpha_{lim}$. Similarly, on the upstroke when $\dot{\phi}(t) < 0$, $\alpha = \alpha_{lim}$. Note that $\alpha = \alpha_{lim}$ on both the upstroke and downstroke because positive α is defined as a counter clockwise rotation for the downstroke and a clockwise rotation for the upstroke. Figure 5 shows the relationships between the right wing spar axis system and the upstroke and downstroke wing fixed coordinate systems. The transformation between the spar and downstroke wing

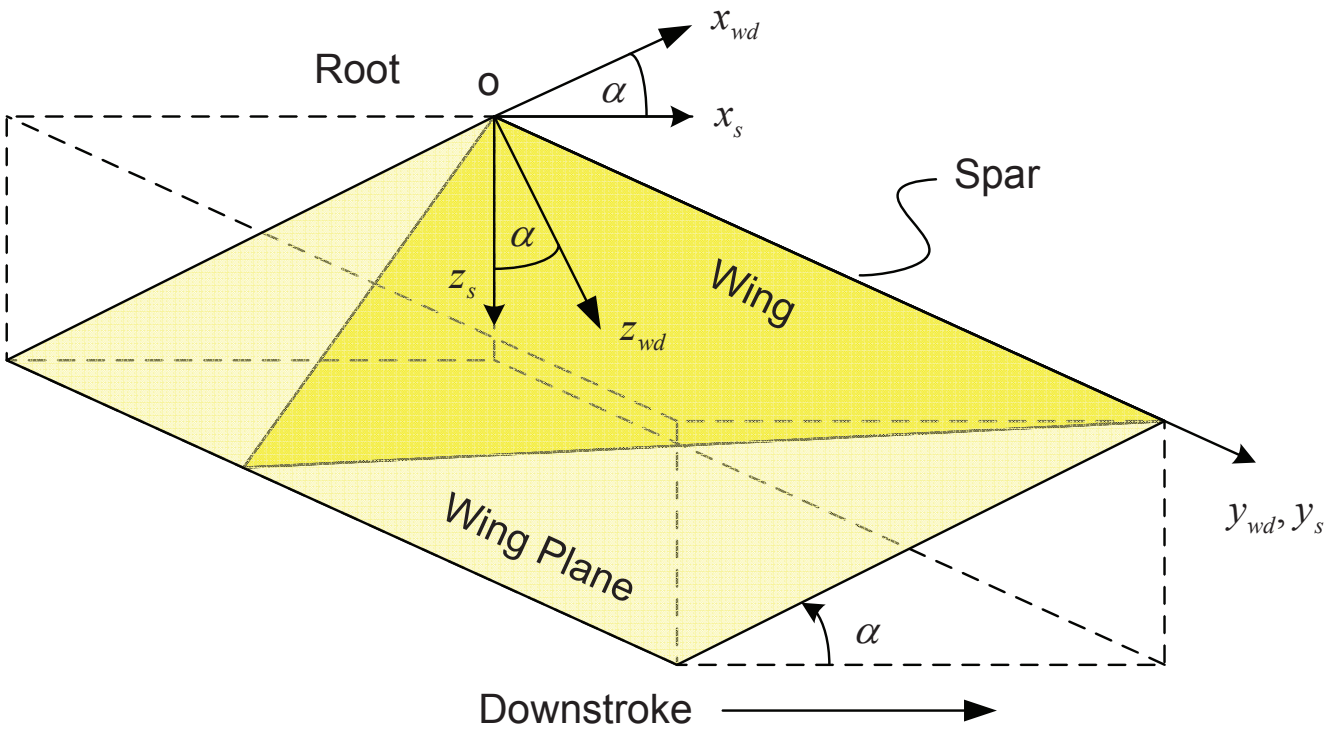

Figure 5. Relationship between right wing and spar axis systems .

coordinate system is defined as

$$\begin{bmatrix} x_{RWS} \\ y_{RWS} \\ z_{RWS} \end{bmatrix} = \begin{bmatrix} \cos\alpha & 0 & \sin\alpha \\ 0 & 1 & 0 \\ -\sin\alpha & 0 & \cos\alpha \end{bmatrix} \begin{bmatrix} x_{RWPD} \\ y_{RWPD} \\ z_{RWPD} \end{bmatrix} \tag{12}$$

While, the transformation between the spar and upstroke wing coordinate system is defined as

$$\begin{bmatrix} x_{RWS} \\ y_{RWS} \\ z_{RWS} \end{bmatrix} = \begin{bmatrix} -\cos\alpha & 0 & \sin\alpha \\ 0 & 1 & 0 \\ -\sin\alpha & 0 & -\cos\alpha \end{bmatrix} \begin{bmatrix} x_{RWPU} \\ y_{RWPU} \\ z_{RWPU} \end{bmatrix} \tag{13}$$

With the relationships between the body, root, spar, upstroke wing, and downstroke wing axis systems established, we may transform the instantaneous values of lift and drag on the wing into the body axis coordinate frame. Recall that lift is defined as the component of aerodynamic force perpendicular to the relative wind, while drag is defined as the component of aerodynamic force parallel to the relative wind. If the air mass is quiescent, then the relative wind is parallel to the stroke plane defined by $x_{RWS} - y_{RWS}$. For the upstroke, the

aerodynamic forces expressed in body axis coordinates are given by

$$\begin{bmatrix} F^B_{RWU_x} \\ F^B_{RWU_y} \\ F^B_{RWU_z} \end{bmatrix} = \mathbf{R}^B_{RWR}\mathbf{R}^{RWR}_{RWS} \begin{bmatrix} D_{RWU} \\ 0 \\ -L_{RWU} \end{bmatrix} = \begin{bmatrix} L_{RWU} \\ -D_{RWU}\sin(\phi) \\ D_{RWU}\cos(\phi)) \end{bmatrix} \tag{14}$$

and for the downstroke

$$\begin{bmatrix} F^B_{RWD_x} \\ F^B_{RWD_y} \\ F^B_{RWD_z} \end{bmatrix} = \mathbf{R}^B_{RWR}\mathbf{R}^{RWR}_{RWS} \begin{bmatrix} -D_{RWD} \\ 0 \\ -L_{RWD} \end{bmatrix} = \begin{bmatrix} L_{RWD} \\ D_{RWD}\sin(\phi) \\ -D_{RWD}\cos(\phi) \end{bmatrix} \tag{15}$$

For the left wing, a wing-root fixed frame $x_{LWR}, y_{LWR}, z_{LWR}$ is defined that is parallel to x_B, y_B, z_B but whose origin is located at the left wing root pivot point. A spar fixed frame, $x_{LWS}, y_{LWS}, z_{LWS}$ is defined that rotates through an angle $\phi(t)$ about the root pivot point. Here, when $\phi(t) = 0$, $z_{LWS} = -x_{LWR}$, y_{LWS} is coincident with the wing spar, positive proximal to distal, and x_{LWS} completes the right handed coordinate system. The transformation between the spar and root axis system is given by

$$\begin{bmatrix} x_{LWR} \\ y_{LWR} \\ z_{LWR} \end{bmatrix} = \begin{bmatrix} 0 & 0 & -1 \\ -\sin\phi(t) & -\cos\phi(t) & 0 \\ -\cos\phi(t) & \sin\phi(t) & 0 \end{bmatrix} \begin{bmatrix} x_{LWS} \\ y_{LWS} \\ z_{LWS} \end{bmatrix} \tag{16}$$

The relationship between the left wing spar axis and left wing planform coordinate system on the downstroke is

$$\begin{bmatrix} x_{LWS} \\ y_{LWS} \\ z_{LWS} \end{bmatrix} = \begin{bmatrix} -\cos\alpha & 0 & \sin\alpha \\ 0 & 1 & 0 \\ -\sin\alpha & 0 & -\cos\alpha \end{bmatrix} \begin{bmatrix} x_{LWPD} \\ y_{LWPD} \\ z_{LWPD} \end{bmatrix} \tag{17}$$

while the transformation between the left wing spar and upstroke left wing planform coordinate system is

$$\begin{bmatrix} x_{LWS} \\ y_{LWS} \\ z_{LWS} \end{bmatrix} = \begin{bmatrix} \cos\alpha & 0 & \sin\alpha \\ 0 & 1 & 0 \\ -\sin\alpha & 0 & \cos\alpha \end{bmatrix} \begin{bmatrix} x_{LWPU} \\ y_{LWPU} \\ z_{LWPU} \end{bmatrix} \tag{18}$$

For the upstroke, the aerodynamic forces from the left wing expressed in body axis coordinates are given by

$$\begin{bmatrix} F^B_{LWU_x} \\ F^B_{LWU_y} \\ F^B_{LWU_z} \end{bmatrix} = \mathbf{R}^B_{LWR}\mathbf{R}^{LWR}_{LWS} \begin{bmatrix} -D_{LWU} \\ 0 \\ -L_{LWU} \end{bmatrix} = \begin{bmatrix} L_{LWU} \\ D_{LWU}\sin(\phi) \\ D_{LWU}\cos(\phi) \end{bmatrix} \tag{19}$$

and for the down stroke

$$\begin{bmatrix} F^B_{LWD_x} \\ F^B_{LWD_y} \\ F^B_{LWD_z} \end{bmatrix} = \mathbf{R}^B_{LWR}\mathbf{R}^{LWR}_{LWS} \begin{bmatrix} D_{LWD} \\ 0 \\ -L_{LWD} \end{bmatrix} = \begin{bmatrix} L_{LWD} \\ -D_{LWD}\sin(\phi) \\ -D_{LWD}\cos(\phi) \end{bmatrix} \tag{20}$$

For the single degree of freedom problem, the cycle averaged force from both wings, in the x_B direction, $\overline{F}^B_x$, is computed. Assuming that the wing is always on the hinge limit when $\dot{\phi}(t) \neq 0$, then $\alpha = \alpha_{lim}$ and for convenience the subscript on α in the subsequent equations is eliminated. By design, the wings beat synchronously, thus $\phi_{LW}(t) = \phi_{RW}(t)$ and $L_{LWU} = L_{LWD} = L_{RWD} = L_{RWU} \triangleq L$ and these subscripts are also eliminated. Equation 10 indicates that the wing angular velocity is cyclic with a frequency of ω and a period of $2\pi/\omega$, thus the cycle averaged force in the body x-axis direction for the left and right wings is given by

$$\overline{F}^B_x = \frac{\omega}{2\pi}\int_0^{\frac{2\pi}{\omega}} F^B_{LWU_x} + F^B_{RWU_x} dt \tag{21}$$

or

$$\overline{F}^B_x = \frac{\omega}{2\pi}\int_0^{\frac{2\pi}{\omega}} 2L(t) dt \tag{22}$$

Substituting Equations 4 and 10 into Equation 22 yields

$$\overline{F}^B_x = \frac{\rho\omega^3}{2\pi} I_A C_L(\alpha) \int_0^{2\pi/\omega} \sin^2(\omega t) dt \tag{23}$$

which reduces to

$$\overline{F}^B_x = \frac{\rho\omega^2}{2} I_A C_L(\alpha) = k_L \omega^2 \tag{24}$$

Note that because the MAV is constrained to flight in one direction $x_I = x_B$. Thus,

$$\overline{F}^I_x = \frac{\rho\omega^2}{2} I_A C_L(\alpha) \tag{25}$$

From Equation 25, the wingbeat frequency that produces a specified cycle-averaged force in

the vertical direction is given by

$$\omega_{F_x} \triangleq \sqrt{\frac{2\overline{F}_x^I}{\rho I_A C_L(\alpha)}} \tag{26}$$

and a trim hover frequency can be computed as

$$\omega_o = \sqrt{\frac{2mg}{\rho I_A C_L(\alpha)}} \tag{27}$$

B. Altitude Control System

If $F_x(t)$ could be manipulated as desired and if sensors are available to measure altitude and altitude rate, a linear control law can be implemented that allows the aircraft to track a desired altitude command. A control law that produces a damped second order response to a desired altitude command, x_{des}, is given by

$$F_x(t) = m(-2\zeta_a\omega_a\dot{x} - \omega_a^2 x + \omega_a^2 x_{des} + g) \tag{28}$$

Of course, $F_x(t)$ cannot be arbitrarily manipulated because it is constrained to be periodic. However, it is postulated that if the bandwidth of the tracking law is much less than the wing beat frequency, i.e. $\omega_a \ll \omega$, then the cycle averaged force $\overline{F_x}$ can be specified and used in place of a perfect x-force generator. The one control variable that we have at our disposal for this problem is the wing beat frequency ω which is related to $\overline{F_x}$ by Equation 26. Figure 6 shows a block diagram of the control law. Note that $2\zeta\omega_a$ and ω_a^2 are design variables and that the feedback controller manipulates the frequency of the oscillator that drives the wing angular position. The "Cycle ZOH" block is an element that takes the instantaneous value

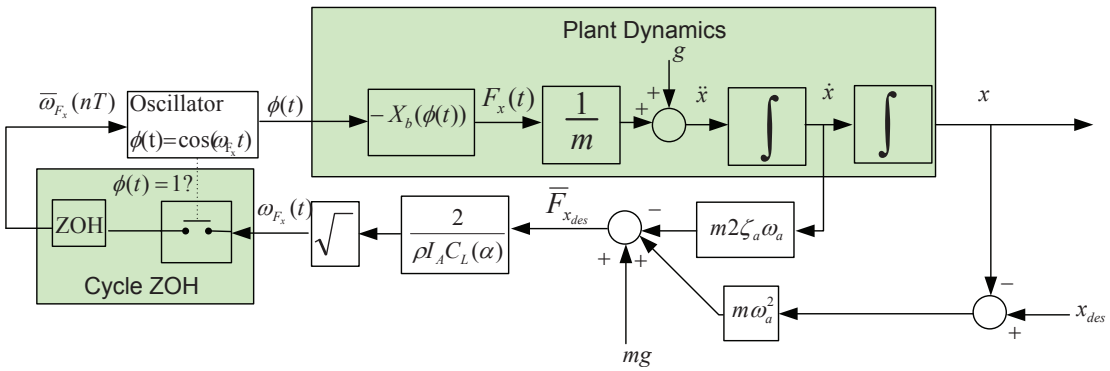

Figure 6. Block Diagram of Altitude Command Tracking Control System.

of the oscillator frequency command signal and holds it constant until the current wingbeat cycle is complete. Its' purpose is to preserve the shape of a cosine wave over each wingbeat cycle. Without such an element, the control law can fundamentally change the shape of the wingbeat position wave form resulting in spikes or other undesired features.

III. Stability of Dynamic Systems Under the Influence of Periodic Control Inputs

In this section, it is desired to analytically determine an expression for the altitude of this system driven by a periodic input. The goal is to gain insight into the problem and to determine limitations of control for these types of systems.

A. Analytical Solution

The point mass, single degree-of-freedom equation-of-motion for a flapping wing micro air vehicle in hover can be written as

$$\ddot{x} = -g + \frac{F_x}{m} \tag{29}$$

where $F_x = 2L = 2k_L\dot{\phi}^2$. The force F_x is an *instantaneous* aerodynamic force generated by the flapping motion of both wings. For this analysis, the angle-of-attack of the wing is assumed to be constant along the entire span on both the upstroke and downstroke, with an instantaneous change in angle-of-attack at the end of each stroke. Thus we are neglecting the rotational dynamics at the end of each upstroke/downstroke where the wing "flips" in order to maintain the same leading edge, and thus a positive angle-of-attack with respect to the mean stroke plane. This approximation is made in order to simplify the analysis.

Equation 29 is a second-order, ordinary differential equation with constant coefficients. The forcing terms are a step function with magnitude g and a harmonic forcing term; therefore, it is rather straight-forward to find an analytical solution to this differential equation. It can be shown that for the initial conditions $\dot{x}(0) = \dot{x}_0$ and $x(0) = x_0$, the solution to

$$\ddot{x}(t) = -g + \frac{2k_L\omega^2}{m}\sin^2\omega t$$

is

$$x(t) = x_0 + \dot{x}_0 t + \left(\frac{-g}{2} + \frac{k_L\omega^2}{2m}\right)t^2 + \frac{k_L}{4m}\left[\cos\left(2\omega\, t\right) - 1\right] \tag{30}$$

Inspection of Equation 30 suggests that if $\dot{x}_0 \equiv 0$, then there is a unique wing beat frequency that will render the solution to be a stable limit cycle that oscillates about x_0 with an amplitude $k_L/(4m)$. The trim frequency is found by forcing the coefficient on the t^2 term to

vanish

$$\frac{-g}{2} + \frac{k_L \omega^2}{2m} = 0 \tag{31}$$

Solving for ω gives the trim frequency

$$\omega_0 = \sqrt{\frac{mg}{k_L}} \tag{32}$$

Thus, for the frequency ω_0 and $\dot{x}_0 = 0$, the vehicle will exhibit a stable limit cycle described by

$$x(t) = x_0 + \frac{k_L}{4m} \left[\cos\left(2\omega\, t\right) - 1\right] \tag{33}$$

with amplitude $k_L/(4m)$ about the point x_0. In this case, for all frequencies $\omega \neq \omega_0$ the coefficient on t^2 will be non-zero; therefore, the limit cycle will be unstable. Note that the trim frequency calculated in Equation 32 is identical to the one calculated in Equation 27, as can be seen by recalling that $k_L = \frac{\rho}{2} I_A C_L(\alpha)$.

IV. Simulation Results

The single degree of freedom altitude command tracking system was simulated in order to evaluate system performance. The vehicle was constrained to move in the x direction only. The vehicle parameters are The trim frequency is equivalent to a value of 120.1742 Hz. The

Table 1. Vehicle Specifications.

Parameter	Value	Units
Mass	60	mg
Width	4	mm
Height	11	mm
Depth	1	mm
b_{wing}	3	mm
$\bar{c}_{wing}$	4	mm
r_{wing}	15	mm
α_U	45	deg
α_D	45	deg
ω_o	755.0569	$\frac{rad}{sec}$
I_A	935	m^4

desired altitude command is a series of step functions of magnitude 1 m. Figure 7 shows

a close-up of altitude for an open-loop simulation. In this case, the left and right wing frequencies were set to ω_0 for all time. The vehicle should exhibit a stable limit cycle given by Equation 33 with $x_0 = 0$. Figure 8 shows the altitude from the simulation as well as the limit cycle from Equation 33. As can be seen, a limit cycle does exist and is accurately predicted by Equation 33.

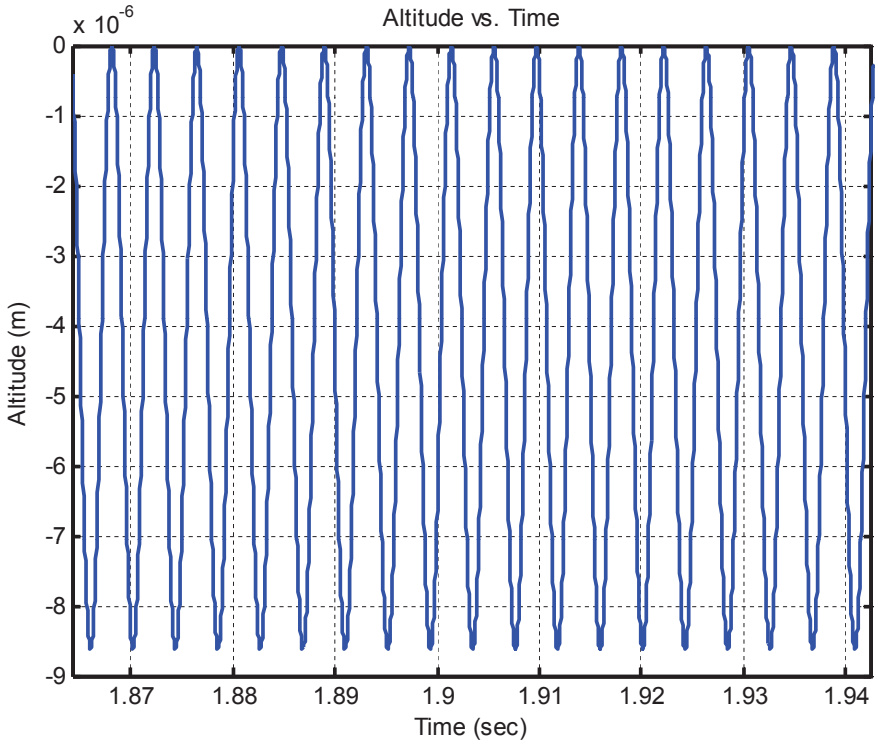

Figure 7. Altitude vs. Time.

Now, the feedback loop is closed and tracking of a reference command is desired. The reference is a series of 1 m step changes in altitude. Figure 9 shows the command and actual altitudes. Clearly, the system is capable of tracking these altitude commands. Recall, the control variables are the fundamental wing beat frequencies of the left and right wing. The left and right wing beat frequencies used to generate the appropriate altitude are shown in Figure 10. Relatively large changes in ω_{LW}, ω_{RW} are necessary in order to track the altitude command. Figures 11 and 12 show the altitude tracking and required wing beat frequency when the desired altitude is a sinusoidal signal of amplitude 0.25 m and a frequency of 5 $\frac{rad}{sec}$. Tracking is acceptable, however, there is quite a variation in wing beat frequency to generate a 0.25 m amplitude sinusoidal wave.

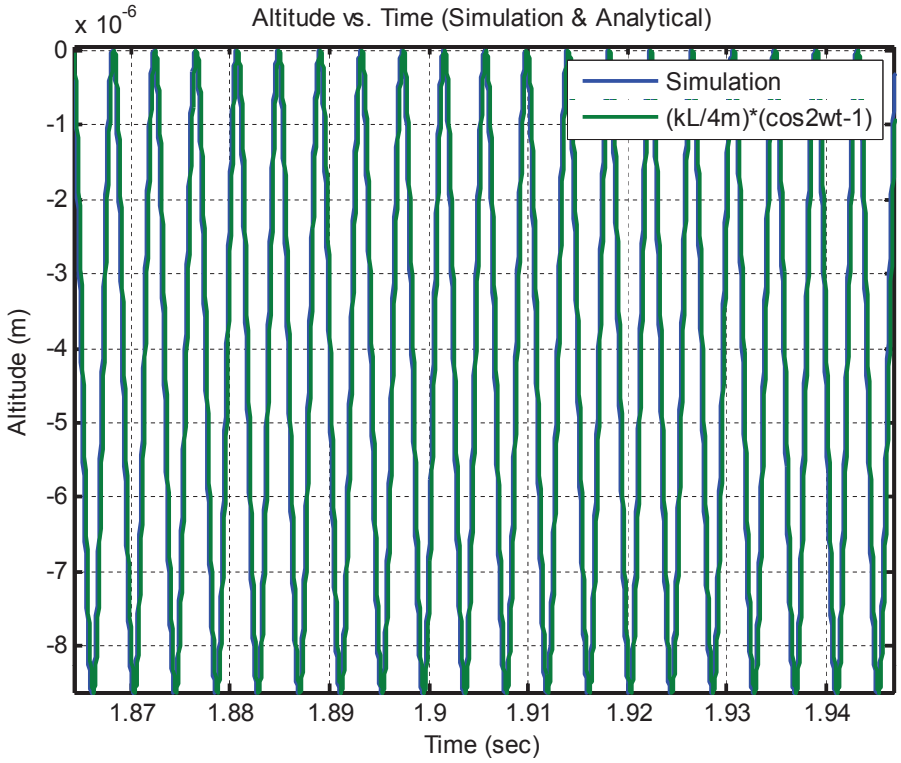

Figure 8. Altitude vs. Time.

V. Summary

In this work, an analysis of the one degree-of-freedom equation of motion was presented. An aerodynamic model was developed using blade element theory. The cycle-averaged force in the inertial x-axis direction (vertical) was computed, from which, a hover frequency was calculated. The point mass single degree-of-freedom equation of motion was solved to yield the altitude time history. A stable limit cycle was achieved with a suitable choice of wing beat frequency, and this frequency was exactly the hover frequency. Results showed that the solution to the single degree-of-freedom equation of motion was identical to that obtained from the full simulation. A control law, that produces a damped second order response to command inputs, was developed. Simulation results show that the performance of the controller is acceptable.

References

[1]Wood, R. J., "The First Takeoff of a Biologically Inspired At-Scale Robotic Insect," *IEEE Transactions on Robotics*, Vol. 24, No. 2, 2007, pp. 341–347.

[2]Doman, D. B., Oppenheimer, M. W., and Sigthorsson, D. O., "Dynamics and Control of a Minimally

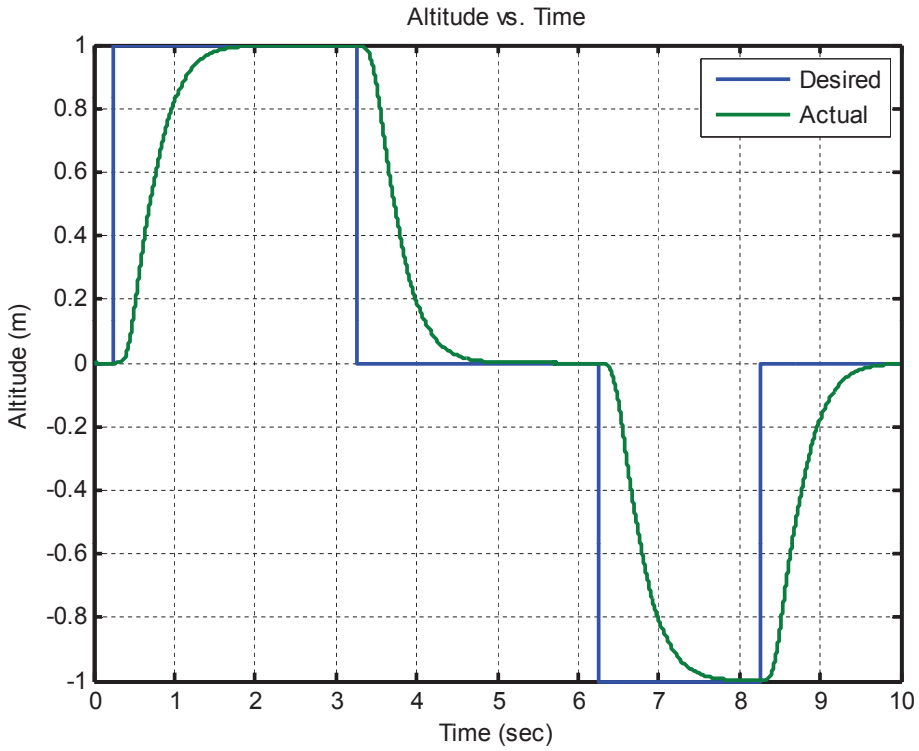

Figure 9. Altitude vs. Time.

Actuated Biomimetic Vehicle. Part I. Aerodynamic Model," Submitted to 2009 AIAA Guidance, Navigation and Control Conference, Aug. 2009.

[3]Oppenheimer, M. W., Doman, D. B., and Sigthorsson, D. O., "Dynamics and Control of a Minimally Actuated Biomimetic Vehicle. Part II. Control," Submitted to 2009 AIAA Guidance, Navigation and Control Conference, Aug. 2009.

[4]Sanjay P. Sane and Michael H. Dickenson, "The Control of Flight Force by a Flapping Wing: Lift and Drag Force Production," *The Journal of Experimental Biology*, Vol. 204, 2001, pp. 2607–2626.

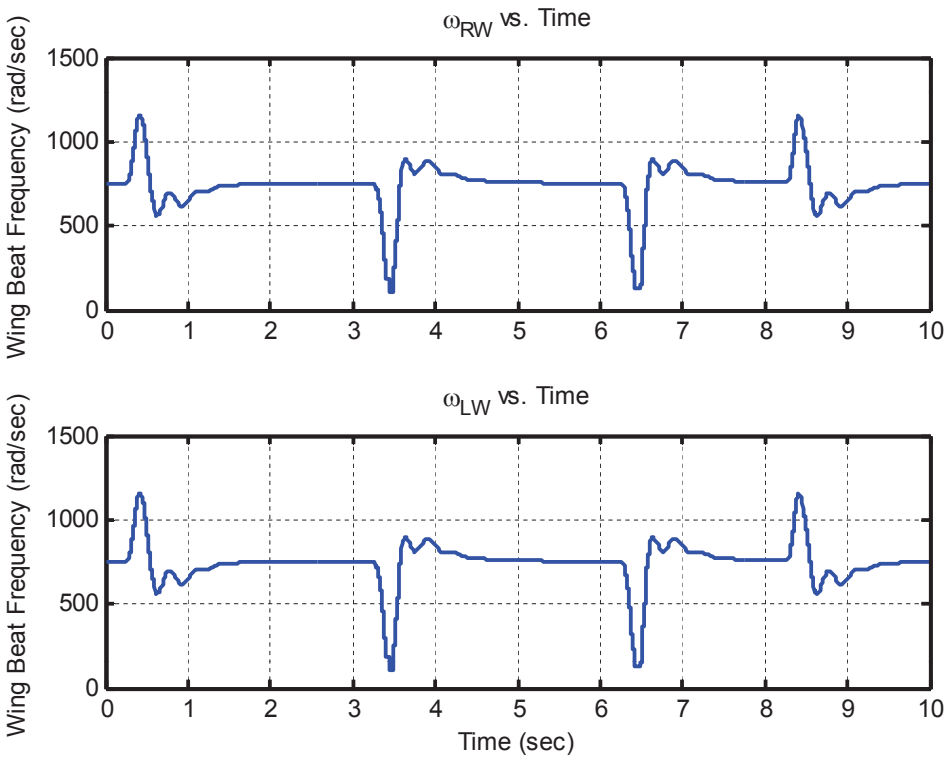

Figure 10. ω vs. Time.

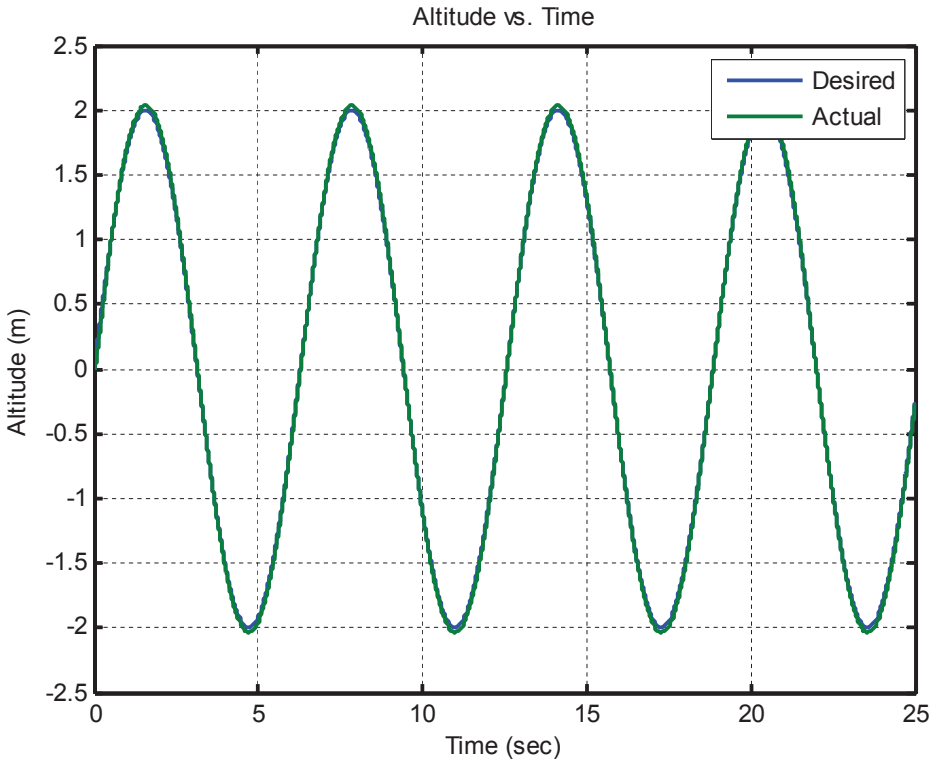

Figure 11. Altitude vs. Time.

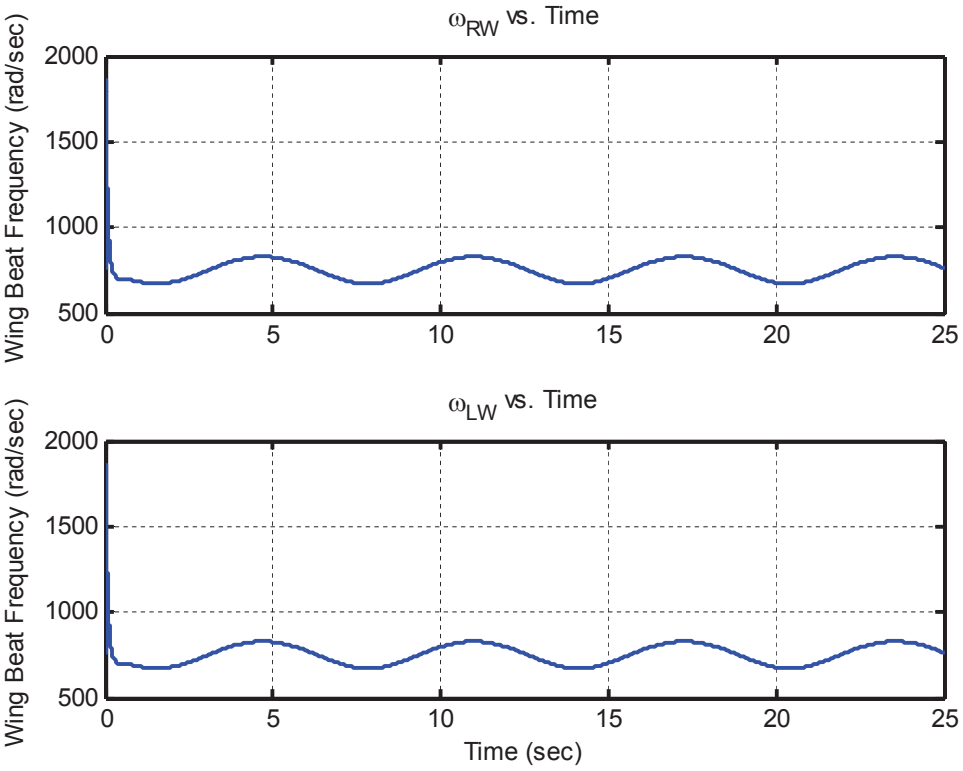

Figure 12. ω vs. Time.